Desalination and Water Treatment
www.deswater.com

doi: 10.1080/19443994.2015.1109560

57 (2016) 19311–19320
September

Taylor & Francis
Taylor & Francis Group

Exploration of calcium doped zinc oxide nanoparticles as selective adsorbent for extraction of lead ion

Sher Bahadar Khan[a,b,*], Hadi M. Marwani[a,b], Abdullah M. Asiri[a,b], Esraa M. Bakhsh[a]

[a]*Faculty of Science, Department of Chemistry, King Abdulaziz University, P.O. Box 80203, Jeddah 21589, Saudi Arabia, Tel. +966 593709796, +966 12 6952293; Fax: +966 12 6952292; email: sbkhan@kau.edu.sa (S.B. Khan), Tel. +966 12 6952293; Fax: +966 12 6952292; emails: hmarwani@kau.edu.sa (H.M. Marwani), aasiri2@kau.edu.sa (A.M. Asiri), ebakhsh0004@stu.kau.edu.sa (E.M. Bakhsh)*

[b]*Center of Excellence for Advanced Materials Research (CEAMR), King Abdulaziz University, P.O. Box 80203, Jeddah 21589, Saudi Arabia*

Received 2 April 2015; Accepted 21 September 2015

ABSTRACT

Ca-doped ZnO nanoparticles-based extraction system has been developed which can be employed simultaneously for the recognition and elimination of Pb(II) ions because of solid interaction among Ca-doped ZnO nanoparticles and Pb(II). The extraction ability of Ca-doped ZnO nanoparticles were deliberated for the removal of lead ions utilizing inductively coupled plasma-optical emission spectrometry. The extraction aptitudes of Ca-doped ZnO were scrutinized for numerous metal ions, comprising Cd(II), Cu(II), Hg(II), La(III), Mn(II), Pb(II), Pd(II), and Y(III). The extraction results revealed that Ca-doped ZnO nanoparticles is selective only for Pb(II). The exclusion ability of Ca-doped ZnO nanoparticles for Pb(II) was 84.66 mg g^{-1}. Furthermore, the extraction profile of Pb(II) on Ca-doped ZnO nanoparticles was matched with the Langmuir adsorption isotherm, which suggest monolayer adsorption of Pb(II) on Ca-doped ZnO nanoparticles. Kinetic study showed that Pb(II) adsorption on Ca-doped ZnO nanoparticles obeyed the pseudo-second-order kinetic model. Calculated thermodynamic parameters also revealed that the adsorption mechanism is a common spontaneous and thermodynamically favorable process. Finally, detection of Pb(II) in environmental water samples was carried out by the anticipated method.

Keywords: Ca-doped ZnO; Nanoparticles; Pb(II); Adsorbent; Water treatment; Environmental applications

1. Introduction

The continuous release of organic pollutants, heavy metals and other contaminants by different industries causing many problems related to human health and aquatic systems [1–3]. These heavy metals generally contaminate ground and surface water and adversely affect the human health by causing different infections and disorders. Metals such as cadmium, chromium, cobalt, lead, and mercury, play crucial role in originating numerous diseases and disorders because of nonbiodegradable nature of metal ions [2]. Thus, heavy metals are considered to be the utmost toxic materials among water pollutants and give considerable harmful threats to the environment [1–3].

*Corresponding author.

Pb(II) is an ecotoxicological hazard and is the main concern because of its poisonous nature, toxicity, and existence in nature [4–6]. Generally, Pb(II) exist in natural water in the range of 2–10 mg mL^{-1} but maximum 10 ng mL^{-1} is mentioned by World Health Organization [7]. Therefore, the toxic nature of Pb(II) has directed to the fabrication of selective and efficient methods for the recognition of Pb(II) ions in the environment. A huge number of techniques have been executed for the assessment of content level of Pb(II) in aqueous media [8–11]. However, due to the lower sensitivity and selectivity of these techniques especially at ultra-trace concentration limits their vast applicability. So, an effective separation technique is needed at priority basis in order to detect, quantify, and extract metal ions in accurate way [12]. Solid-phase extraction is one of the superior techniques due to cost, selectivity, effectiveness, and less solvent usage [13,14].

Different materials such as silica, polymer, alumina, and ion-imprinted materials have been utilized for different metal ions adsorption [15–20]. Among these materials, ion-imprinted materials are appropriate and favorable for the selective extraction of metal ions but it is difficult to collect and separate ion-imprinted materials from the solution after the sorption process. On the other side, metal oxide nanomaterials are easy to collect and separate from the solution after the sorption process, and therefore, metal oxide nanomaterials have created substantial attention because of their prospective application in metal ion extraction [1]. Metal oxide nanomaterials have peculiar and copious applications concerning human health as it impart substantially to medicine and environment. Nanomaterials exhibit a unique competence to extract metal ion that is rarely possible regarding conservative systems [1]. Nanomaterials possess specific shape, trivial size, high surface area, and extraordinary surface activity. ZnO has got attention because of its extensive applications, such as catalysis, sensor, use in rubber, plastic, cosmetics, coating, and electronic devices [21]. Zinc oxide has versatile applications but it still needs improvement in order to enhance its properties. Among different techniques, one is doping of nanomaterials known to reveal outstanding properties in numerous areas. Dopants increase the surface area, reduce the mass and alter the morphologies of the nanomaterials resulting in much improved assets of nanomaterials [22–25].

Therefore, we prepared Ca-doped ZnO nanoparticles and FESEM, EDS, X-ray diffraction (XRD), FTIR, XPS, and UV were used for their structure elucidation. Ca-doped ZnO nanoparticles were applied for the extraction of metal ion, such as Cd(II), Cu(II), Hg(II), La(III), Mn(II), Pb(II), Pd(II), and Y(III) and was found to be highly selective for Pb(II). The adsorption process for Pb(II) was found to be monolayer adsorption with adsorption capacity of 84.66 mg g^{-1}.

2. Experimental

2.1. Chemicals and reagents

All the chemicals used for experiments were purchased from Sigma-Aldrich (Milwaukee, WI, USA).

2.2. Synthesis of Ca-doped ZnO nanoparticles

Ca-doped ZnO was prepared by similar procedure as reported in the literature [22–25]. The required quantity of calcium carbonate and zinc chloride were added to 100 ml of double-distilled water and prepare 0.1 M solution of each salt. The solution was then made basic with pH 10 by adding 0.5 M NaOH solution and kept on stirring at 60.0°C for overnight. The mixture was filtered and the precipitate was washed. The washed product was dried and calcined at 400.0°C for 5 h.

2.3. Metals extraction

First, a specific concentration (2 mg L^{-1}) of each metal ion was prepared. The pH of all metal ion solution was attuned to 5.0 by using acetate buffer. For extraction analysis, 25 mg of Ca-doped ZnO nanoparticles were added to each metal ion solution. For adsorption capacity analysis, we prepared different Pb (II) solutions of 0, 5, 10, 15, 20, 25, 30, 50, 100, 125, and 150 mg L^{-1}, set the pH 5.0 of each solution and added 25 mg Ca-doped ZnO nanoparticles in each solution. All the mixed solutions were shaken by mechanical shaker for 1 h at 150 rpm and room temperature. Ca-doped ZnO were shaken at different time (2.5, 5, 10, 20, 30, 40, 50, and 60 min) using 100 mg L^{-1} Pb(II) solution in order to evaluate the influence of shaking time on adsorption. Thermodynamic parameters were determined at 278, 298, 313, and 338 K using 5 mg L^{-1} Pb(II) solution.

2.4. Apparatus

The particle size of Ca-doped ZnO was examined by JEOL Scanning Electron Microscope (JSM-7600F, Japan) while EDS from Oxford was used for checking the elements. The structure of synthesized product was elucidated from XRD patterns analysis, FTIR and XPS spectra recorded by Thermo scientific XRD (ARL

service), Thermo scientific FTIR (iS50) and Thermo Scientific XPS (K-Alpha KA1066 spectrometer). The optical properties were evaluated from UV spectrum using Thermo Scientific UV–vis spectrophotometer (Evolution^{TM} 300). The ICP-OES spectrometer (Perkin Elmer ICP-OES model Optima 4100 DV, USA) was utilized with parameters given elsewhere [1–3].

3. Results and discussion

3.1. Structure elucidation of Ca-doped ZnO nanoparticles

FESEM was used for morphology evaluation of Ca-doped ZnO and the images are depicted in Fig. 1. FESEM images revealed that Ca-doped ZnO is grown in the shape of particles and the grown particles are aggregated with each other. The average diameter of grown Ca-doped ZnO nanoparticles is almost ~50 nm.

The compositional analysis of nanoparticles was assessed by utilizing EDS and is portrayed as Fig. 2. The EDS displayed peaks at 0.3 and 3.7 eV which correspond to Ca, peak at 1.1 eV appeared for Zn and another peak at 0.5 eV is due to oxygen that suggests the presence of Ca, Zn, and oxygen elements in the synthesized nanoparticles. EDS displayed 89.98 wt% of oxygen, 9.86 wt% of Zn and only 0.15 wt% of Ca suggesting that ZnO has been doped by Ca. No other element was traced out suggesting pure Ca-doped ZnO nanoparticles.

Fig. 3 shows comparison of XRD spectrum of Ca-doped ZnO with pure ZnO (red color) pattern. The low intense peak appeared at $2\theta = 23.03$, 29.50, 39.48, 43.24, 45.56, 48.74, 57.50, 60.88 indicating the presence of $CaCO_3$ in the samples [26]. All other peaks appeared for ZnO are compatible with wurtzite hexagonal zinc oxide [27,28]. The intense peaks appeared for ZnO in XRD patterns of nanoparticles clearly display that nanoparticles are mainly composed of ZnO phase. The relative content of $CaCO_3$ phase is low while for the ZnO phase, the diffraction peaks are stronger. These results indicate that the synthesized nanoparticles are Ca-doped ZnO.

Ca-doped ZnO nanoparticles revealed peaks in FTIR spectrum for metal oxygen at 530, 1,359, 1,635, and 3,397 cm^{-1} (Fig. 3(b)). The strong peak that appeared at 530 cm^{-1} was ascribed to M=O or M–O–M (M = Zn, Ca) bond whereas the extra peaks that appeared at 1,359 are ascribed to CO_3 anion used during the synthesis process. The moisture peaks are shown at 1,635 and 3,397 cm^{-1} [27,28].

X-ray photoelectron spectroscopy was also analyzed for Ca-doped ZnO nanoparticles in order to confirm their composition (Fig. 4). XPS revealed peaks for Ca $2p_{3/2}$, O 1s and Zn $2p_{1/2}$ at binding energies of 341.1, 530.1, and 1,071.6 eV, respectively which are compatible with the literature [22,29]. The slight shift in binding energy of Ca and Zn might be due to the doping effect.

The optical properties of Ca-doped ZnO nanoparticles were analyzed and the UV–vis graph is displayed in Fig. 5(a). UV–vis spectrum revealed an absorption peak at 300 nm for Ca-doped ZnO nanoparticles whereas the band gap energy was found to be 3.0 eV which is deliberated using $(\alpha h\nu)^{1/n}$ vs. $h\nu$ plots (Fig. 5(b)) by Tauc's formula [24,25].

3.2. Removal of Pb(II) on Ca-doped ZnO nanoparticles

3.2.1. Sensitivity and selectivity of Ca-doped ZnO nanoparticles

The developed Ca-doped ZnO nanoparticles are selective for Pb(II) in the presence of other interfering metal ions which is one the key advantage of the fabricated Ca-doped ZnO nanoparticles [30]. To investigate the influence of other interfering metal ions exist along with Pb(II) ions in surrounding environment or wastewater, selectivity of Ca-doped ZnO nanoparticles

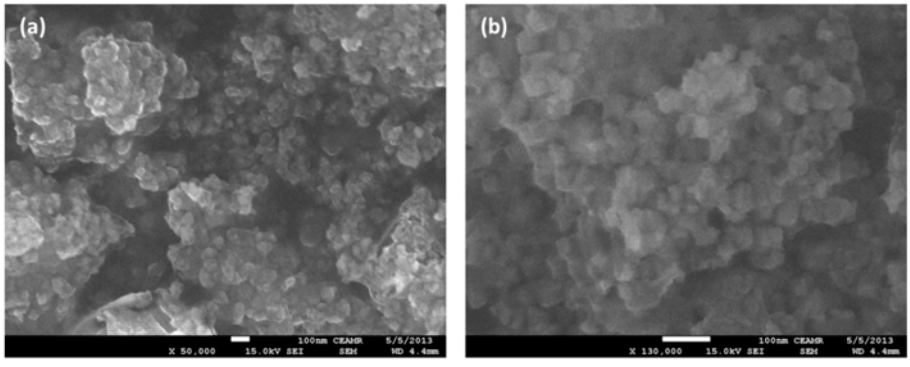

Fig. 1. Typical (a) low-magnification and (b) high-resolution FESEM images of Ca-doped ZnO nanoparticles.

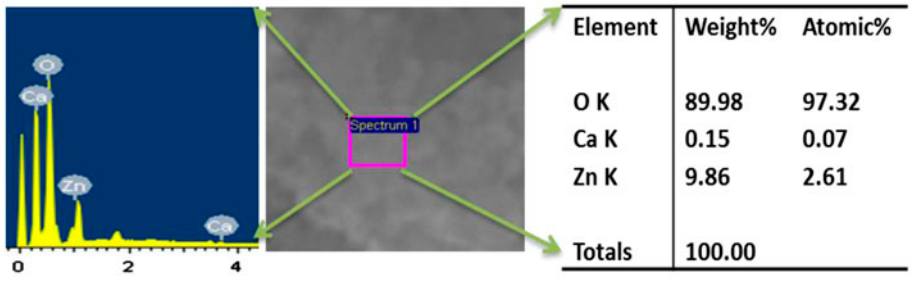

Fig. 2. Typical EDS spectrum of Ca-doped ZnO nanoparticles.

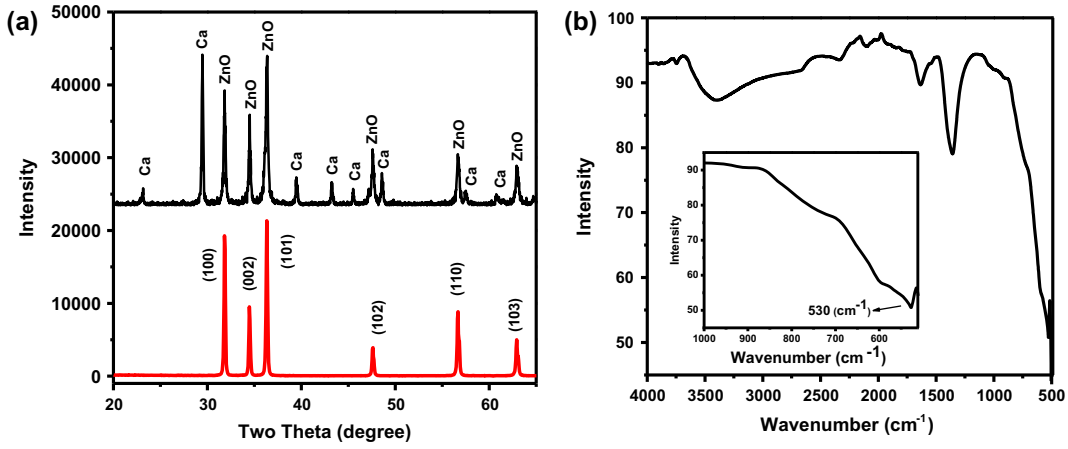

Fig. 3. Typical XRD pattern (a) and FTIR spectrum (b) of Ca-doped ZnO nanoparticles.

for various metal ions were explored based on the distribution coefficient of Ca-doped ZnO nanoparticles. The distribution coefficient (K_d) was acquired from Eq. (1) [1]:

$$K_d = (C_o - C_e/C_e) \times (V/m) \quad (1)$$

where C_o is the initial and C_e is the final concentrations, V is the volume (mL), and m is the weight of Ca-doped ZnO nanoparticles (g) [1]. The distribution coefficient obtained for each metal ions is given in Table 1, which clearly indicate the maximum value for Pb(II) ions with Ca-doped ZnO nanoparticles among all metal ions. The quantity of Pb(II) was practically all bind and removed by Ca-doped ZnO nanoparticles. Hence, selectivity investigation specified that Ca-doped ZnO nanoparticles are highly selective only for Pb(II) ions rather than other metal ions. Based on the above results, one can suggest electrostatic attraction or a chelating mechanism of adsorption (Fig. 6). The high binding and extraction behavior of Ca-doped ZnO nanoparticles suggest that there is not much interference of other metal ions and the developed system based on Ca-doped ZnO nanoparticles is more selective in nature.

The designed sensitive and innovative Ca-doped ZnO is extremely simple system and approach for the recognition and extraction of Pb(II) ions. The Ca-doped ZnO nanoparticles pronounced simple and cheap method devoid of any sophisticated technique or further modification. The mechanism of the designed system is based on the interaction of Ca-doped ZnO nanoparticles with Pb(II) ions and this binding led to the complete removal of Pb(II) ions by a simple filtration (Fig. 6). The surface of metal oxides becomes anionic in nature by dispersing in water and also cause upsurge in surface area [31]. We have used Ca-doped ZnO nanoparticles for the removal of Pb(II) ion, having small particle size and large active surface area because particle size and surface area perform a significant part related to accessibility and adsorption capability. Small particle size and large active surface area also increases the binding capability of nanomaterials which results in high performance of recognition and simultaneous elimination of Pb(II) ions. The high sensitivity and selectivity of fabricated Ca-doped ZnO

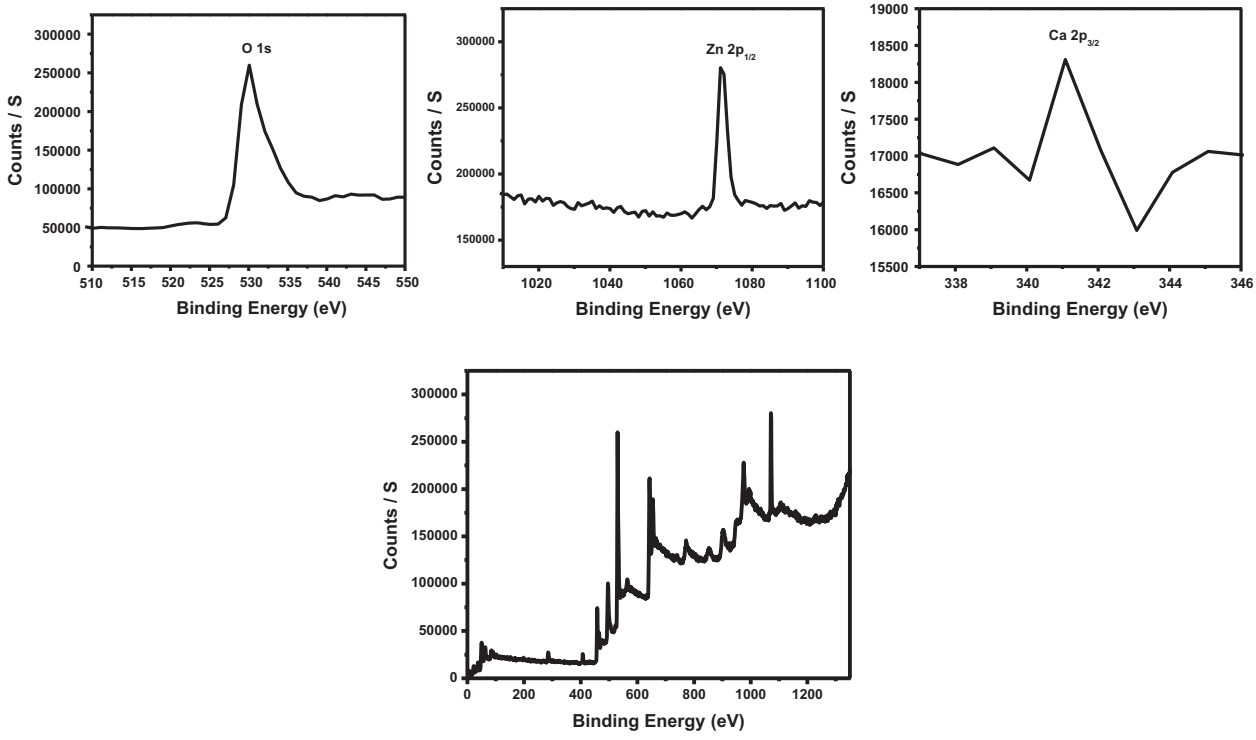

Fig. 4. Typical XPS spectrum of Ca-doped ZnO nanoparticles.

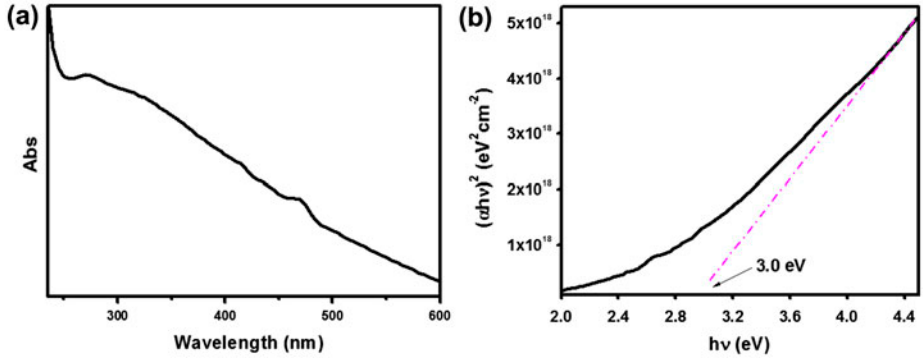

Fig. 5. UV–vis spectrum (a) and $(\alpha h\nu)^2$ vs. $h\nu$ plot (b) of Ca-doped ZnO nanoparticles.

nanoparticles toward Pb(II) ions may be due to the fact that Ca-doped ZnO nanoparticles affords fast channeling or movement of Pb(II) ions for proficient binding of metal ions and simultaneously superb adsorbing behavior of Ca-doped ZnO nanoparticles.

3.2.2. Sensing, static adsorption, and removal capacity of Pb(II) ions

The uptake capacity was carried out for Ca-doped ZnO nanoparticles in order to study the performance and removal efficiency as a function of Pb(II) ions concentration. In view of the advantages of Ca-doped ZnO nanoparticles in sensing and adsorption application, we have tested the performance of Ca-doped ZnO nanoparticles toward diverse concentrations of Pb(II) ions at pH 5. 25 mL of Pb(II) solutions (concentrations from 0 to 150 mg L^{-1}) were separately mixed with Ca-doped ZnO nanoparticles (25 mg) and carried out mechanically shaking for 1 h. The adsorption capacity of Ca-doped ZnO toward metal ion was obtained using Eq. (2) as follows:

Table 1
Selectivity study of Ca-doped ZnO nanoparticles adsorption towards different metal ions at pH 5.0 and 25°C ($N = 3$)

Metal ion	q_e (mg g^{-1})	K_d (mL g^{-1})
Pb(II)	2.00	5.67×10^5
Cu(II)	1.60	3.96×10^3
Cd(II)	1.37	2.16×10^3
Mn(II)	1.28	1.77×10^3
Hg(II)	1.20	1.51×10^3
Y(III)	1.19	1.45×10^3
Pd(II)	0.89	8.03×10^2
La(III)	0.46	2.99×10^2

$$q_e = \frac{(C_o - C_e)V}{m} \quad (2)$$

where q_e is the adsorbed Pb(II) on Ca-doped ZnO nanoparticles (mg g^{-1}), C_o is the initial concentrations of Pb(II) in solution (mg L^{-1}), C_e is the equilibrium concentrations of metal ion in solution (mg L^{-1}), V is the volume (L) and m is the weight of Ca-doped ZnO nanoparticles (g). Fig. 7(a) and (c) demonstrates the uptake capacity of Ca-doped ZnO and its sensitivity towards Pb(II). As can be seen, up to 20 mg L^{-1} of Pb (II) ions, there is a gradual increase in uptake capacity of Ca-doped ZnO nanoparticles reaching to maximum, indicates complete attachment of Pb(II) with Ca-doped ZnO nanoparticles. As the amount of Pb(II) increases, the removal efficiency of Ca-doped ZnO nanoparticles also increases. Adsorption capacity of Ca-doped ZnO nanoparticles for Pb(II) was 84.66 mg g^{-1}. It has been observed that 25 mg of Ca-doped ZnO nanoparticles removed almost all Pb(II) ions showing the highly efficient nature of Ca-doped ZnO nanoparticles. From the above results it is quite clear that Ca-doped ZnO nanoparticles based system has high removal efficiency for the extraction of Pb(II) ions. The adsorption capacity of Ca-doped ZnO nanoparticles for Pb(II) is better than reported for Pb(II) (49.9 [32], 54.48 [33], 90.25 [34], and 97.08 mg g^{-1} [35]).

3.3. Adsorption isotherm models

The removal of Pb(II) by Ca-doped ZnO nanoparticles was evaluated by Langmuir equation given in Eq. (3) to understand equilibrium isotherm [36]:

$$\frac{C_e}{q_e} = \left(\frac{C_e}{Q_o}\right) + \frac{1}{Q_o b} \quad (3)$$

where C_e is the concentrations of Pb(II) ion (mg mL^{-1}) and q_e relates to the adsorbed Pb(II) ion by Ca-doped ZnO nanoparticles (mg g^{-1}). Q_o and b represent Langmuir constants related to adsorption capacity (mg g^{-1}) and energy of adsorption (L mg^{-1}), respectively.

The plot of C_e/q_e vs. C_e give slope and intercept which are equal to $1/Q_o$ and $1/Q_o b$, respectively. Further, the crucial features of Langmuir adsorption isotherm is constant separation factor or equilibrium parameter, R_L, that is $R_L = 1/(1 + bC_o)$, where b is Langmuir constant that specifies behavior of adsorption and character of isotherm; C_o denotes Pb(II) initial concentration. The R_L value gives suggestion about the kind of adsorption, and R_L values from 0 to 1 signify a favorable adsorption [37–40].

The adsorption behavior of Pb(II) ion on Ca-doped ZnO nanoparticles was fit better with Langmuir equation (Fig. 7(c)) suggesting that the adsorption process follow Langmuir adsorption isotherm model, which recommend monolayer adsorption of Pb(II) ion

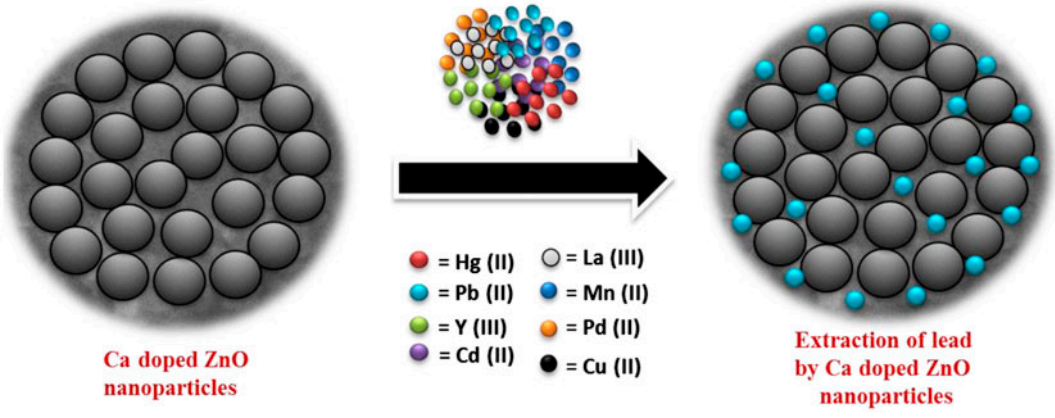

Fig. 6. Schematic view of adsorption profile of Pb(II) on the surface of Ca-doped ZnO nanoparticles.

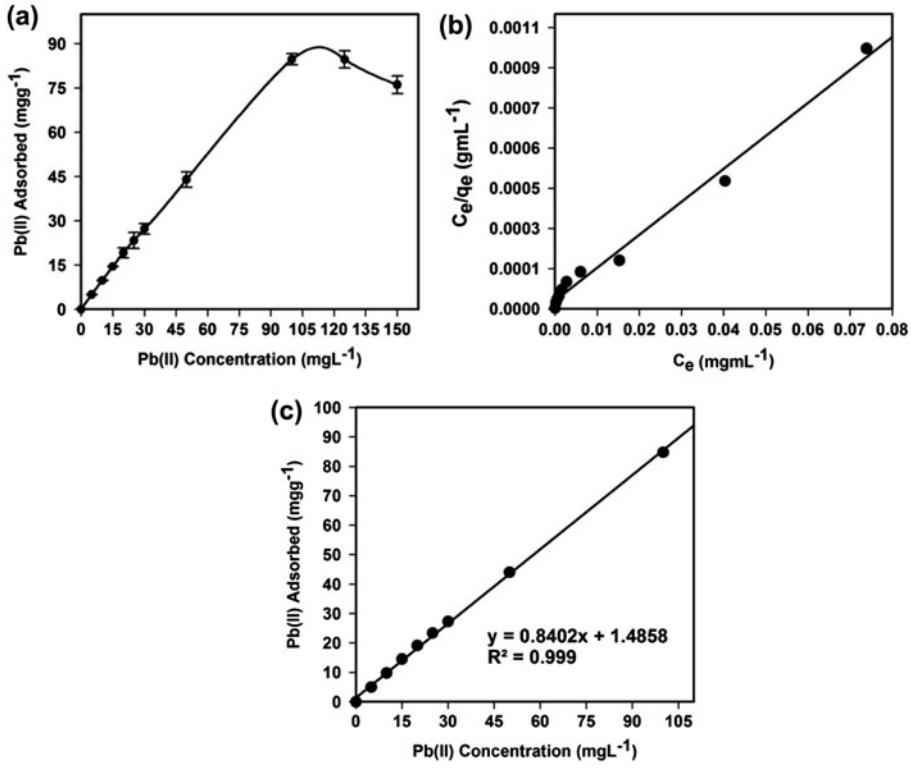

Fig. 7. (a) Adsorption profile of Pb(II) and (b) Langmuir adsorption isotherm model of Pb(II) adsorption on 25 mg of Ca-doped ZnO nanoparticles at pH 5.0 and 25˚C, and (c) sensitivity of sensor. Adsorption experiments were obtained at different concentrations (0–150 mg L^{-1}) of Pb(II) under static conditions.

on Ca-doped ZnO nanoparticles. Langmuir constants Q_o and b is equal to 81.19 mg g^{-1} and 0.41 L mg^{-1} while the correlation coefficient is $R^2 = 0.989$ for Pb(II) adsorption on Ca-doped ZnO nanoparticles. The uptake capacity (81.19 mg g^{-1}) achieved from Langmuir equation is closely in agreement with experimental value (84.66 mg g^{-1}). The R_L value for the adsorption of Pb(II) on Ca-doped ZnO nanoparticles is 0.02, suggesting an extremely favorable adsorption phenomena.

3.4. Effect of contact time

The influence of contact time was studied for evaluating the time required to attain equilibrium and confirming the possibility for applications of Ca-doped ZnO nanoparticles to selectively bind Pb(II). The batch method was implemented using 100 mg L^{-1} Pb(II) and different (2.5–60.0 min) contact times (Fig. 8(a)). Fig. 8(a) shows that the Pb(II) adsorption onto Ca-doped ZnO nanoparticles is highly dependent on the contact time. The amount of Pb(II) adsorption increase greatly with increase in contact time till it reached the highest adsorption capacity after 60 min. These results suggested that equilibrium kinetics for the adsorption of Ca-doped ZnO nanoparticles for Pb(II) was extremely fast.

3.5. Kinetic models

Several kinetic models were used for estimating kinetic adsorption parameters and pseudo-second-order kinetic model (Eq. (4)) was applied to the experimental data and measured different parameters.

$$\frac{t}{q_t} = \frac{1}{\upsilon_o} + \left(\frac{1}{q_e}\right)t \tag{4}$$

where $\upsilon_o = k_2 q_e^2$ is the preliminary adsorption rate (mg g^{-1} min^{-1}) and k_2 (g mg^{-1} min^{-1}) denotes the adsorption rate constant, q_e (mg g^{-1}) represents the amount of Pb(II) adsorbed at equilibrium, and q_t (mg g^{-1}) corresponds to the amount of Pb(II) on the surface of Ca-doped ZnO at time t (min). The parameters q_e and υ_o can be obtained from the slope and intercept, respectively, of a plot of t/q_t vs. t [41].

Pseudo-second-order model was nicely fit to the experimental adsorption data suggesting that Pb(II)

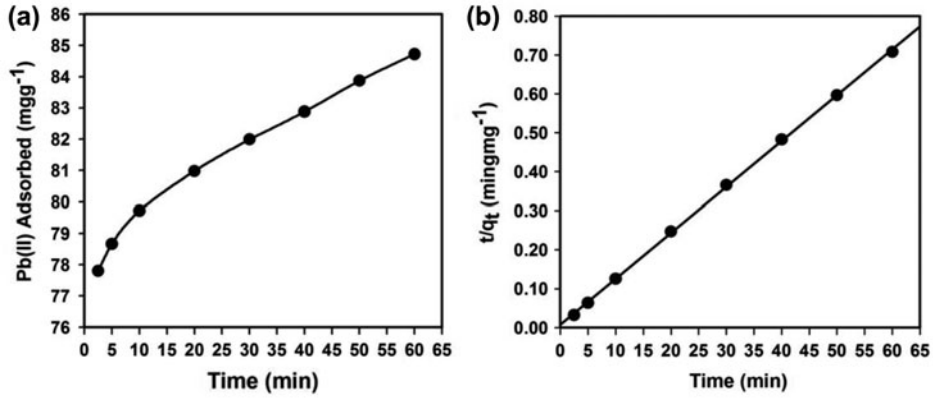

Fig. 8. (a) Effect of contact time on the adsorption of 100 mg L^{-1} Pb(II) and (b) pseudo-second-order adsorption kinetic model of Pb(II) uptake on 25 mg Ca-doped ZnO nanoparticles at pH 5.0 and 25°C.

adsorption on Ca-doped ZnO obeys pseudo-second-order kinetic (Fig. 8(b)). The R^2 value (0.9997) suggests that pseudo-second-order fit nicely as compared to other kinetic models. Parameters v_o, q_e and k_2 were calculated to be 137.31 mg g^{-1} min^{-1}, 84.87 mg g^{-1} and 0.02 g mg^{-1} min^{-1}, respectively. The q_e value is consistent with those acquired from adsorption isotherm experiments and Langmuir adsorption isotherm model, strongly support that Pb(II) adsorption form a monolayer on the surface of Ca-doped ZnO.

3.6. Effect of temperature

The adsorption of 25 mg Ca-doped ZnO nanoparticles towards 5 mg L^{-1} Pb(II) was investigated at 278, 298, 313, and 338 K and their thermodynamic parameters were estimated. K_d (distribution adsorption coefficient) was calculated from Eq. (1). In addition, the slope and intercept of plot ln K_d vs. $1/T$ using Eq. (5) gave standard enthalpy change (ΔH°, kJ mol^{-1}) and standard entropy change (ΔS°, J mol^{-1} K^{-1}), as reported in Table 2.

$$\ln K_d = \frac{\Delta S^\circ}{R} - \left(\frac{\Delta H^\circ}{RT}\right) \quad (5)$$

where R denotes the universal gas constant (8.314 J mol^{-1} K^{-1}), and T refers to the temperature in Kelvin. Further, the standard Gibbs free energy change (ΔG°, kJ mol^{-1}) described in Table 2 was determined from Eq. (6):

$$\Delta G^\circ = \Delta H^\circ - T\Delta S^\circ \quad (6)$$

As shown in Table 2, calculated values of ΔH°, ΔS°, and ΔG° are all negative. The observed negative ΔH° value provides that the adsorption behavior is exothermic. In addition, negative values of ΔG° indicates that the adsorption process of Ca-doped ZnO nanoparticles towards Pb(II) is a general spontaneous process and thermodynamically favorable. The negative ΔS° reveals that degree of freedom decreases at the solid–liquid interface during the adsorption of Pb (II) on Ca-doped ZnO nanoparticles.

3.7. Application of the proposed method to environmental water samples

The designed system was implemented for the detection and extraction of Pb(II) in real-water samples such as drinking water, lake water, seawater, and tap water, collected from Jeddah in Saudi Arabia. The % extraction of Pb(II) in real-water samples (Table 3) was in the range of 94.40–99.00%. Thus, the designed system looks feasible and trustworthy for trace analysis of environmental water samples.

Table 2
Estimated thermodynamic parameters of 5 mg L^{-1} Pb(II) adsorption on 25 mg Ca-doped ZnO nanoparticles (N = 3)

		ΔG° (kJ mol^{-1})			
ΔH° (kJ mol^{-1})	ΔS° (J mol^{-1} K^{-1})	T = 278 K	T = 298 K	T = 313 K	T = 338 K
−76.30	−149.85	−34.56	−32.27	−28.52	−25.98

Table 3
Determination of Pb(II) at different concentrations (1, 3, and 12 mg L^{-1}) in real-water samples using 25 mg Ca-doped ZnO nanoparticles ($N = 3$)

Samples	Unadsorbed (mg L^{-1})	Extraction (%)
Tap water	0.02	98.50
	0.10	96.66
	0.45	96.24
Lake water	0.02	98.10
	0.11	96.25
	0.53	95.57
Seawater	0.02	97.64
	0.13	95.50
	0.67	94.40
Drinking water	0.01	99.00
	0.05	98.33
	0.35	97.13

4. Conclusions

Highly insightful adsorption system has been fabricated by preparing Ca-doped ZnO nanoparticles. Ca-doped ZnO nanoparticles were structurally elucidated using diverse spectroscopic methods. The designed Ca-doped ZnO nanoparticles-based system could be utilized for simultaneous removal of the Pb(II) ions. The developed system is more selective and there is no significant effect of interfering cations confirming the highly selective nature of Ca-doped ZnO nanoparticles. Sensible static adsorption capacities of 84.66 mg g^{-1} for Ca-doped ZnO nanoparticles were attained for Pb(II) and the adsorption isotherm of Pb (II) was fit to the Langmuir model. The proposed method confirmed that Ca-doped ZnO nanoparticles were effective for a selective adsorption toward Pb(II) following pseudo-second-order kinetic model. Based on estimated thermodynamic parameters, the mechanism of Pb(II) adsorption is concluded to be spontaneous and thermodynamically favorable.

Acknowledgement

The authors are grateful to the Chemistry Department and Center of Excellence for Advanced Materials Research (CEAMR) at King Abdulaziz University for providing research facilities.

References

[1] H.M. Marwani, M.U. Lodhi, S.B. Khan, A.M. Asiri, Selective extraction and determination of toxic lead based on doped metal oxide nanofiber, J. Taiwan Inst. Chem. Eng. 51 (2015) 34–43.
[2] S.B. Khan, J.W. Lee, H.M. Marwani, K. Akhtar, A.M. Asiri, J. Seo, A.A.P. Khan, H. Han, Polybenzimidazole hybrid membranes as a selective adsorbent of mercury, Composites Part B 56 (2014) 392–396.
[3] J.W. Lee, S.B. Khan, H.M. Marwani, K. Akhtar, A.M. Asiri, M.T.S. Chani, J. Seo, H. Han, Development of composite membranes as selective adsorbent for yttrium ion, Int. J. Electrochem. Sci. 8 (2013) 12028–12036.
[4] S. Karabulut, A. Karabakan, A. Denizli, Y. Yürüm, Batch removal of copper(II) and zinc(II) from aqueous solutions with low-rank Turkish coals, Sep. Purif. Technol. 18 (2000) 177–184.
[5] N. Chiron, R. Guilet, E. Deydier, Adsorption of Cu(II) and Pb(II) onto a grafted silica: Isotherms and kinetic models, Water Res. 37 (2003) 3079–3086.
[6] T.K. Naiya, A.K. Bhattacharya, S.K. Das, Adsorption of Cd(II) and Pb(II) from aqueous solutions on activated alumina, J. Colloid Interface Sci. 333 (2009) 14–26.
[7] P.K. Tewari, A.K. Singh, Preconcentration of lead with Amberlite XAD-2 and Amberlite XAD-7 based chelating resins for its determination by flame atomic absorption spectrometry, Talanta 56 (2002) 735–744.
[8] A. Nasu, S. Yamauchi, T. Sekine, Solvent extraction of copper(I) and (II) as thiocyanate complexes with tetrabutylammonium ions into chloroform and with trioctylphosphine oxide into hexane, Anal. Sci. 13 (1997) 903–911.
[9] G.H. Tao, Z. Fang, dual stage preconcentration system for flame atomic absorption spectrometry using flow injection on-line ion-exchange followed by solvent extraction, Fresenius J. Anal. Chem. 360 (1998) 156–160.
[10] M. Soylak, N.D. Erdogan, Copper(II)–rubeanic acid coprecipitation system for separation–preconcentration of trace metal ions in environmental samples for their flame atomic absorption spectrometric determinations, J. Hazard. Mater. 137 (2006) 1035–1041.
[11] J.L. Manzoori, H. Abdolmohammad-Zadeh, M. Amjadi, Simplified cloud point extraction for the preconcentration of ultra-trace amounts of gold prior to determination by electrothermal atomic absorption spectrometry, Microchim. Acta 159 (2007) 71–78.
[12] K. Pyrzyńska, Recent developments in the determination of gold by atomic spectrometry techniques, Spectrochim. Acta, Part B 60 (2005) 1316–1322.
[13] S.A. Ahmed, Alumina physically loaded by thiosemicarbazide for selective preconcentration of mercury(II) ion from natural water samples, J. Hazard. Mater. 156 (2008) 521–529.
[14] A.M. Alvarez, J.R.E. Alvarez, R.P. Alvarez, Heavy metal analysis of rainwaters: A comparison of TXRF and ASV analytical capabilities, J. Radioanal. Nucl. Chem. 273 (2007) 427–433.
[15] H.J. Cho, S.W. Myung, Determination of cadmium, chromium and lead in polymers by ICP-OES using a high pressure asher (HPA), Bull. Korean Chem. Soc. 32 (2011) 489–497.
[16] C. Gustavo Rocha de, A. Ilton Luiz de, R. Paulo dos Santos, Synthesis, characterization and determination of the metal ions adsorption capacity of cellulose modified with p-aminobenzoic groups, J. Mater. Res. 7 (2004) 329–334.

[17] Y. Liu, L. Guo, L. Zhu, X. Sun, J. Chen, Removal of Cr (III, VI) by quaternary ammonium and quaternary phosphonium ionic liquids functionalized silica materials, Chem. Eng. J. 158 (2010) 108–114.
[18] N.S. Awwad, H.M.H. Gad, M.I. Ahmad, H.F. Aly, Sorption of lanthanum and erbium from aqueous solution by activated carbon prepared from rice husk, Colloids Surf., B 81 (2010) 593–599.
[19] P. Biparva, M.R. Hadjmohammadi, Selective separation/preconcentration of silver ion in water by multiwalled carbon nanotubes microcolumn as a sorbent, Clean—Soil, Air, Water 39 (2011) 1081–1086.
[20] H.-Y. Shen, Z.-X. Chen, Z.-H. Li, M.-Q. Hu, X.-Y. Dong, Q.-H. Xia, Controlled synthesis of 2,4,6-trichlorophenol-imprinted amino-functionalized nano-Fe_3O_4-polymer magnetic composite for highly selective adsorption, Colloids Surf., A 481 (2015) 439–450.
[21] S.B. Khan, M.M. Rahman, H.M. Marwani, A.M. Asiri, K.A. Alamry, An assessment of zinc oxide nanosheets as a selective adsorbent for cadmium, Nanoscale Res. Lett. 8 (2013) 377–385.
[22] S.A.B. Asif, S.B. Khan, A.M. Asiri, Efficient solar photocatalyst based on cobalt oxide/iron oxide composite nanofibers for the detoxification of organic pollutants, Nanoscale Res. Lett. 9 (2014) 510–518.
[23] S.A.B. Asif, S.B. Khan, A.M. Asiri, Visible light functioning photocatalyst based on Al_2O_3 doped Mn_3O_4 nanomaterial for the degradation of organic toxin, Nanoscale Res. Lett. 10 (2015) 355–364.
[24] S.A. Khan, S.B. Khan, A.M. Asiri, Core–shell cobalt oxide mesoporous silica based efficient electro-catalyst for oxygen evolution, New J. Chem. 39 (2015) 5561–5569.
[25] S.B. Khan, K.S. Karimov, M.T.S. Chani, A.M. Asiri, K. Akhtar, N. Fatima, Impedimetric sensing of humidity and temperature using CeO_2–Co_3O_4 nanoparticles in polymer hosts, Microchim. Acta 182 (2015) 2019–2026.
[26] N. Tangboriboon, R. Kunanuruksapong, A. Sirivat, Preparation and properties of calcium oxide from eggshells via calcination, Mater. Sci.-Poland 30 (2012) 313–322.
[27] M. Faisal, S.B. Khan, M.M. Rahman, A. Jamal, A.M. Asiri, M.M. Abdullah, Synthesis, characterizations, photocatalytic and sensing studies of ZnO nanocapsules, Appl. Surf. Sci. 258 (2011) 672–677.
[28] M. Faisal, S.B. Khan, M.M. Rahman, A. Jamal, A.M. Asiri, M.M. Abdullah, Smart chemical sensor and active photo-catalyst for environmental pollutants, Chem. Eng. J. 173 (2011) 178–184.
[29] D.B. Lee, L.S. Hong, Y.J. Kim, Effect of Ca and CaO on the high temperature oxidation of AZ91D Mg alloys, Mater. Trans. 49 (2008) 1084–1088.
[30] M. Faisal, A.A. Ismail, F.A. Harraz, H. Bouzid, S.A. Al-Sayari, A. Al-Hajry, Mesoporous TiO_2 based optical sensor for highly sensitive and selective detection and preconcentration of Bi(III) ions, Chem. Eng. J. 243 (2014) 509–516.
[31] D.M. Han, G.Z. Fang, X.P. Yan, Preparation and evaluation of a molecularly imprinted sol–gel material for on-line solid-phase extraction coupled with high performance liquid chromatography for the determination of trace pentachlorophenol in water samples, J. Chromatogr. A 1100 (2005) 131–136.
[32] Z. Li, X. Chang, X. Zou, X. Zhu, R. Nie, Z. Hu, R. Li, Chemically-modified activated carbon with ethylenediamine for selective solid-phase extraction and preconcentration of metal ions, Anal. Chim. Acta 632 (2009) 272–277.
[33] Z. Zang, Z. Hu, Z. Li, Q. He, X. Chang, Synthesis, characterization and application of ethylenediamine-modified multiwalled carbon nanotubes for selective solid-phase extraction and preconcentration of metal ions, J. Hazard. Mater. 172 (2009) 958–963.
[34] H.M. Marwani, M.U. Lodhi, S.B. Khan, A.M. Asiri, Cellulose-lanthanum hydroxide nanocomposite as a selective marker for detection of toxic copper, Nanoscale Res. Lett. 9 (2014) 466–474.
[35] Y.-H. Li, J. Ding, Z. Luan, Z. Di, Y. Zhu, C. Xu, D. Wu, B. Wei, Competitive adsorption of Pb^{2+}, Cu^{2+} and Cd^{2+} ions from aqueous solutions by multiwalled carbon nanotubes, Carbon 41 (2003) 2787–2792.
[36] I. Langmuir, The constitution and fundamental properties of solids and liquids. Part I. Solids, J. Am. Chem. Soc. 38 (1916) 2221–2295.
[37] G. McKay, H.S. Blair, J.R. Gardner, Adsorption of dyes on chitin. I. Equilibrium studies, J. Appl. Polym. Sci. 27 (1982) 3043–3057.
[38] H.M. Marwani, E.M. Bakhsh, H.A. Al-Turaif, A.M. Asiri, S.B. Khan, Enantioselective separation and detection of D-phenylalanine based on newly developed chiral ionic liquid immobilized silica gel surface, Int. J. Electrochem. Sci. 9 (2014) 7948–7964.
[39] S.B. Khan, H.M. Marwani, J. Seo, E.M. Bakhsh, K. Akhtar, D. Kim, A.M. Asiri, Poly(propylene carbonate)/exfoliated graphite nanocomposites: Selective adsorbent for the extraction and detection of gold(III), Bull. Mater. Sci. 38 (2015) 327–333.
[40] S.B. Khan, M.M. Rahman, A.M. Asiri, H.M. Marwani, S.M. Bawaked, K.A. Alamry, Co_3O_4 co-doped TiO_2 nanoparticles as a selective marker of lead in aqueous solution, New J. Chem. 37 (2013) 2888–2893.
[41] Y. Ho, Second-order kinetic model for the sorption of cadmium onto tree fern: A comparison of linear and non-linear methods, Water Res. 40 (2006) 119–125.